TECHNICAL MEMORANDUM

101

Predictability studies with the ECMWF model for the extended range: the impact of horizontal resolution and boundary layer forcing

U. Cubasch and A.C. Wiin Nielsen

Research Department

May 1985

European Centre for Medium-Range Weather Forecasts
Europäisches Zentrum für mittelfristige Wettervorhersage
Centre européen pour les prévisions météorologiques à moyen

Abstract

Experimental 60 day forecasts have been run from observed data using the ECMWF operational model with different resolutions. Even though the mean flow becomes too zonal with all resolutions, there still appears to be usable information beyond day 10 in the forecasts. A more realistic sea surface temperature (SST) generally improves the forecasts in the long run. There are occasions when after a period of low predictive skill the forecast recovers and reaches a level of skill similar to that found short range forecasts. The fact that this happens in the cases with the more realistic SST indicates that it must be more than mere coincidence.

CONTENTS

1. INTRODUCTION

There is a growing body of evidence that in the long term mean the sea surface temperatue (SST) influences the mid-latitude flow pattern (Cubasch, 1984; Shukla and Wallace, 1983). On the other hand, medium range forecasts show only a small response in mid-latitudes to changes of the SST (Arpe and Wallace, 1982). While the climate sensitivity studies had been carried out with low resolution models (typically T21 or R15), the predictability studies have been performed with much finer resolution models (i.e. N48). In this study we shall investigate the extent to which the horizontal resolution influences the impact of the SST on the forecast in the extended range, i.e. the transition period between a direct forecast and a climate simulation (days 10 to 60).

After a brief description of the model and the data used in these experiments (Sections 2.1 and 2.2), the long term mean flow patterns of the atmosphere will be discussed (Section 3.1). This is followed by a suggestion about how extended range forecasts can be objectively verified (Section 3.2). After this, two case studies will be discussed (Sections 4.1 and 4.2).

2. THE EXPERIMENT

2.1 The model

The model used for all experiments is the operational ECMWF spectral model (spring 1984); for further details see Fig. 1. It has been integrated up to 60 days for the following horizontal resolutions: T21, T42 and T63 (i.e. triangular spectral truncation up to zonal wavenumber 21, 42 and 63). In all cases there were 16 levels in the vertical. All the models have been run with the same physical parametrisation, which includes the diurnal cycle in the radiation calculations. All boundary fields were kept at their

$A_{k+\frac{1}{2}}$ (mb)	$B_{k+\frac{1}{2}}$
0	0
50	0
99	0.002
142	0.013
173	0.042
191	0.094
194	0.170
182	0.268
157	0.384
125	0.511
89	0.638
54	0.756
26	0.856
8	0.929
0	0.973
0	0.992
0	1

Vertical Coordinate Table (NL=16)

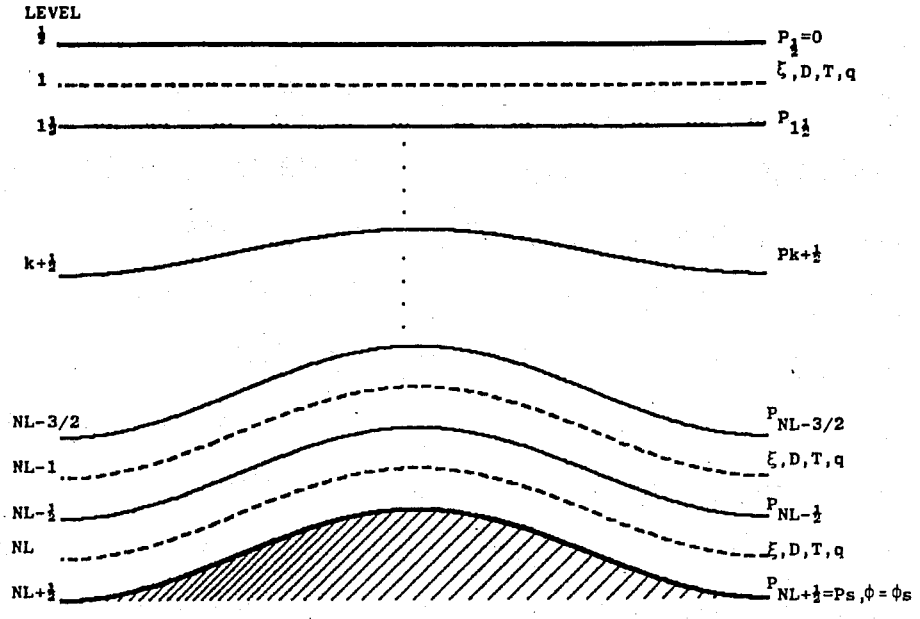

Disposition of variables in the vertical

	T21	T42	T63
Horizontal resolution Δx	5.625°	2.8125°	1.875°
Time step Δt	2400s	1600s	1080s

Dependent variables	ξ,D,T,q,ln(ps)
Vertical coordinate	Hybrid, $P_{k+\frac{1}{2}}=A_{k+\frac{1}{2}}+B_{k+\frac{1}{2}}Ps$, details as above.
Vertical representation	Finite-difference, energy and angular-momentum conserving.
Horizontal representation	Spectral, with triangular truncation at wavenumber 63.
Horizontal grid	96x192 points on a quasi-regular ($\simeq 1.875^{o}$) "Gaussian"grid.
Time integration	Leapfrog, semi-implicit (Δt=20 min), time filter (V=0.06).
Horizontal diffusion	Linear, fourth-order ($K=2\times10^{15}\ m^{4}\ s^{-1}$).
Orography	Grid-scale average from high resolution data set, enhanced by $\sqrt{2}\times$(standard deviation of sub grid-scale orography), spectrally-fitted.
Vertical boundary conditions	Kinematic.
Physical parameterisation	(i) Boundary eddy fluxes dependent on local roughness length and stability (Monin Obukov).
	(ii) Free-atmosphere turbulent fluxes dependent on mixing length and Richardson number.
	(iii) Kuo convection scheme.
	(iv) Interaction between radiation and model-generated clouds. Albedo dependent on model snow cover.
	(v) Large-scale condensation when grid-square saturated. Evaporation of precipitation.
	(vi) Computed land temperature, no diurnal cycle.
	(vii) Computed soil moisture and snow cover.
	(viii) Fixed, analysed sea-surface temperature.

Fig.1: The ECMWF operational forecast model.

initial value. Contrary to the operational forecasts, the orography used in these experiments was the "mean" orography (Tibaldi and Geleyn, 1981).

2.2 The data

The model runs were started from observed initial data in both sets of experiments.

The initial data for the first experiment was provided by the FGGE analysis. These data fall in the same time period as the one used by Bengtsson(1981) for a case study of blocking. Two cases were run:

(a) the SST was set to its climatological values (Alexander and Mobley, 1974);

(b) the SST was set to the 10 day mean value observed at the end of January and the beginning of February 1979 (FGGE data).

The second experiment was started from operationally assimilated data for 1 January 1983, which coincided with the mature phase of the El Nino. Three cases were run:

(a) with the climatological SST;

(b) with the climatological SST plus the observed SST anomaly in the central Pacific for January 1983 (Reynolds, 1984);

(c) with the climatological SST minus the observed SST anomaly in the central Pacific for January 1983 (Reynolds, 1984);

Case (c) was performed in order to find out the extent to which an incorrect SST influences the forecast quality and to gain a better estimate of the natural variability of the model atmosphere.

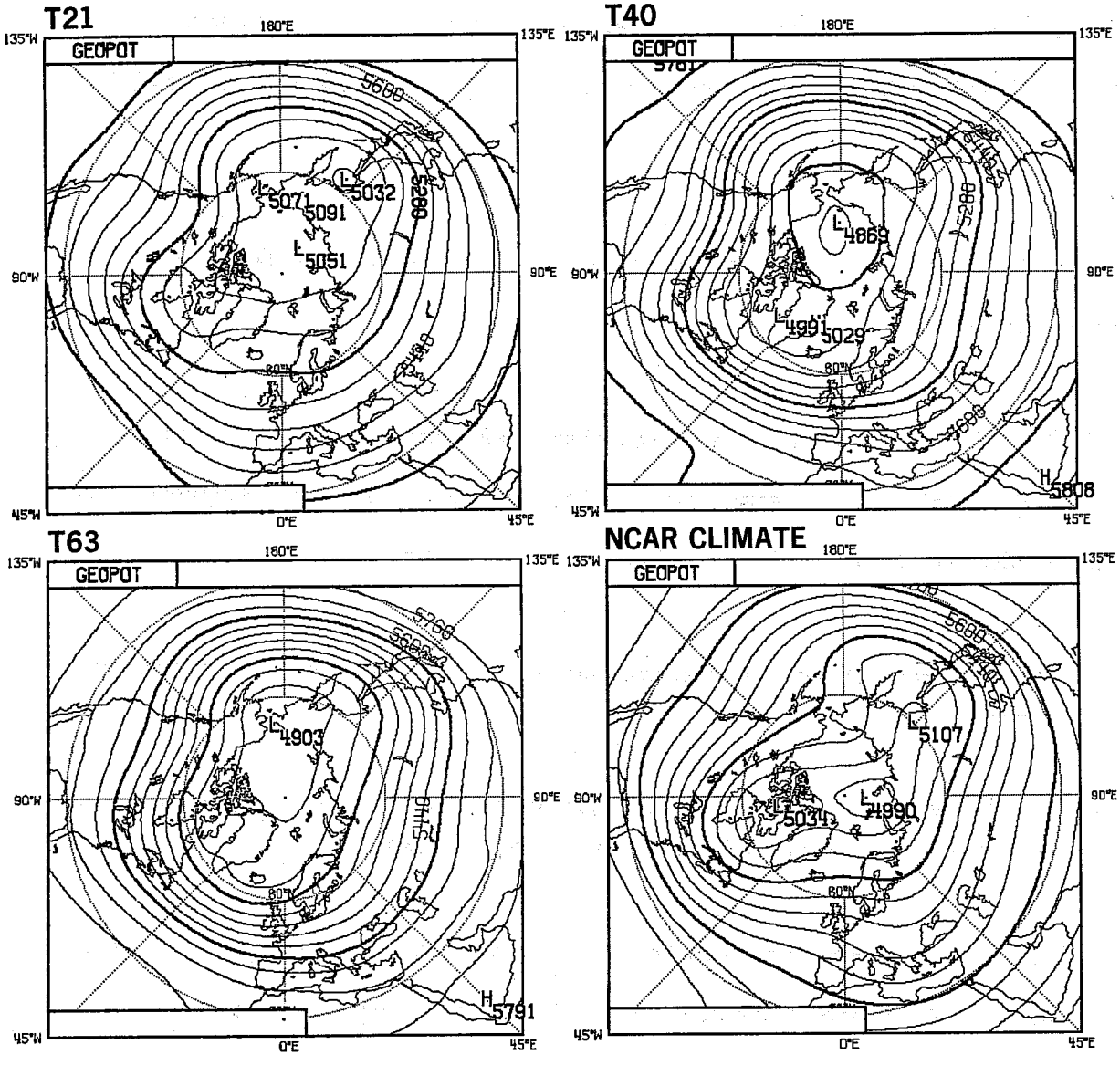

Fig.2: The mean 500 mb height field (contour interval - 80 m).

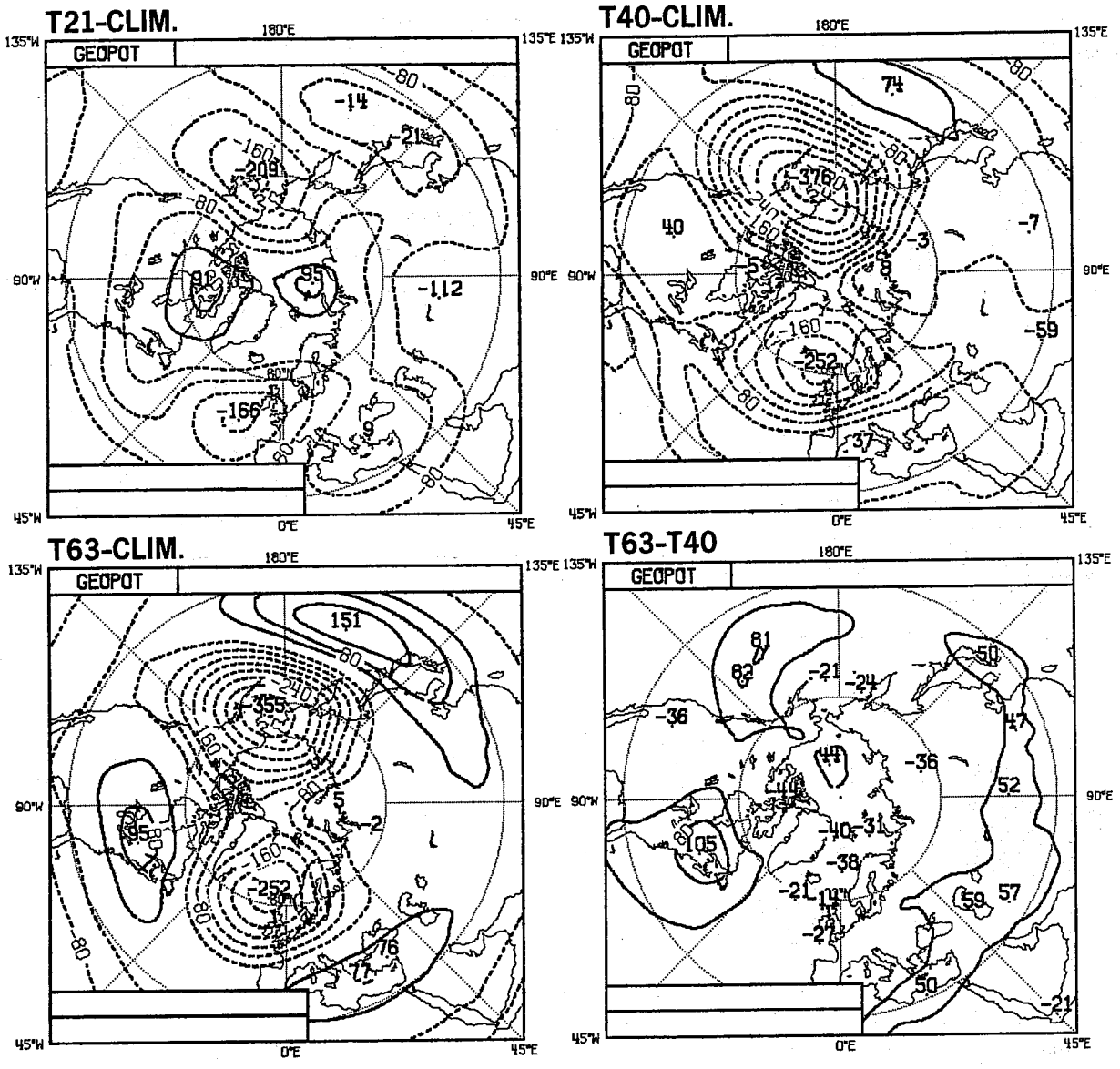

Fig.3: The difference of the 500 mb height field from the observed January climate for different horizontal resolutions (contour interval - 40 m).

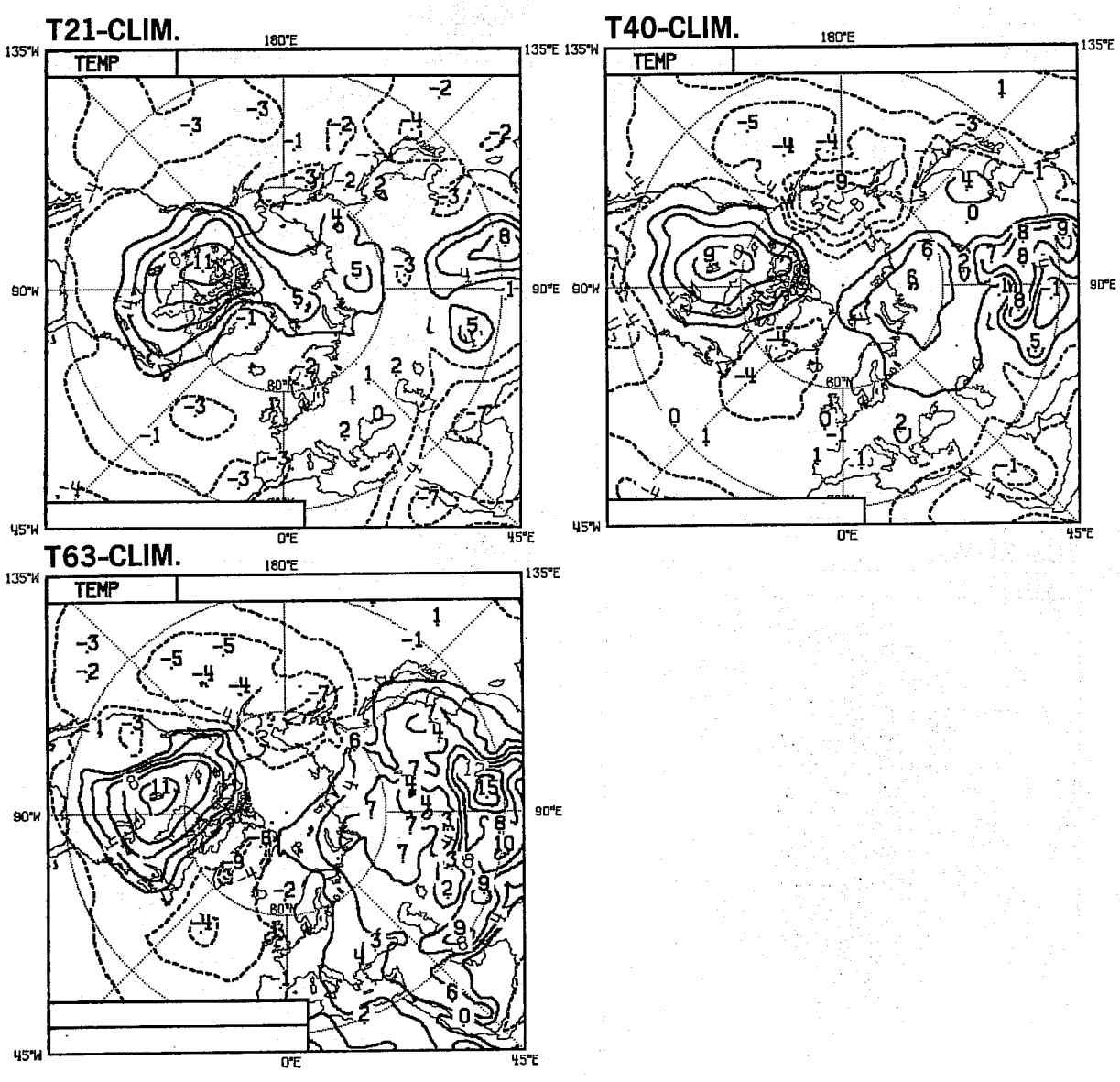

Fig.4: The difference between the 850 mb temperature and the observed January climate for different horizontal resolutions (contour interval - 2°C).

3. EVALUATION

3.1 The mean behaviour of the model atmosphere

A factor which limits the predictability in the extended range has been the tendency of the model flow to become too zonal (Fig.2). This behavoiur seems to be independent of the model type, but dependent on the model resolution (v. Storch et al., 1984). Fig. 3 shows the deviation of the model climate from that observed during January for different model resolutions. The flow pattern for T21 and T40 have been obtained from integrations lasting several years performed with the predecessor of the current operational model (for further details see v. Storch et al, 1984). The T63 field has been obtained by averaging all days beyond day 30 for all T63 runs analysed in this study. The difference between the climate of the old and new model at the same resolution appears to be small. However the difference between the model flow and that observed is quite large for all resolutions, and it increases rapidly when going from T21 to T40; between T40 and T63 this increase is fairly small.

The zonalization tends to obscure any information still contained in an extended range forecast. Therefore it appears to be advantageous to compare anomaly pattern rather than the actual fields.

Contrary to what is found for the height field, the temperature field error hardly alters with increased resolution (Fig. 4). Note that the temperature is overestimated over the land and underestimated over the sea .

3.2 Objective verification of extended range forecasts

Besides the anomaly correlation for daily forecasts (Hollingsworth et al., 1980), a 10 day mean anomaly correlation has been used to objectively verify the results in the mid-latitudes (20.5°N to 82.5°N). This particular

correlation is defined in terms of of 10 day means instead of 1 day values. The calculation of the 10 day mean skill scores is based on datasets truncated at T21. A truncation at a lower wavenumber would give higher scores, but does not alter the relative score between different experiments.

Since it is not known at which threshold a 10 day mean forecast can still be considered useful, and since there exist no indications whether the 60% threshold used to define the limit of usefulnes for a single day correlation has any meaning for 10 day mean forecasts, a limit of skill has been derived from multi-year climate forecasts: It was achieved by asking how much skill the model climate posesses in predicting the 10 day means in the period considered for this predictability study. The correlation coefficients for these 10 day periods (12 cases) have been averaged and to this mean value has been added 1.96 times the standard deviation. The resulting value gives an indication of what correlation coefficient could be achieved just by chance by the model climate. Any value higher than this threshold would be generated by chance by the model climate in only 2.5% of the cases. Due to the similarity of the T40 and the T63 climate, the T40 climate has been used to define the threshold value for the T63 experiments as well. It was felt that using the T63 climate is inappropriate, since it is not independent because it is based on the experiments discussed here.

4. RESULTS

The experiments will be discussed separately.

4.1 The FGGE case

This period was originally selected because a warm SST anomaly stretched from the West African coast to the Caribbean Islands (Fig. 5), and this might have been responsible for the severe winter conditions in Europe during this time.

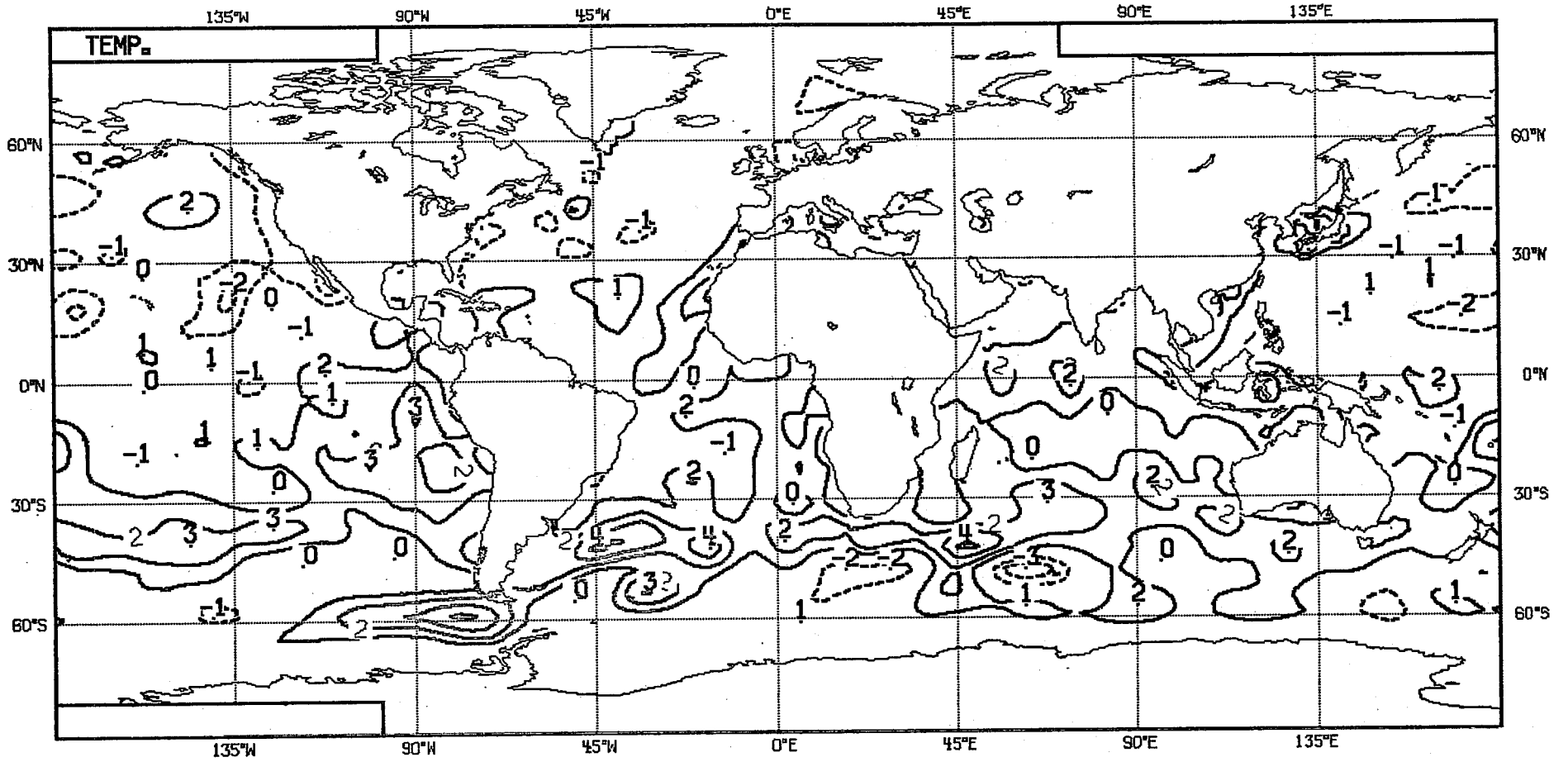

Fig.5: The difference between the observed sea surface temperature during the first 10 days of February 1979 and the climatological February sea surface temperature (contour interval - 1°C).

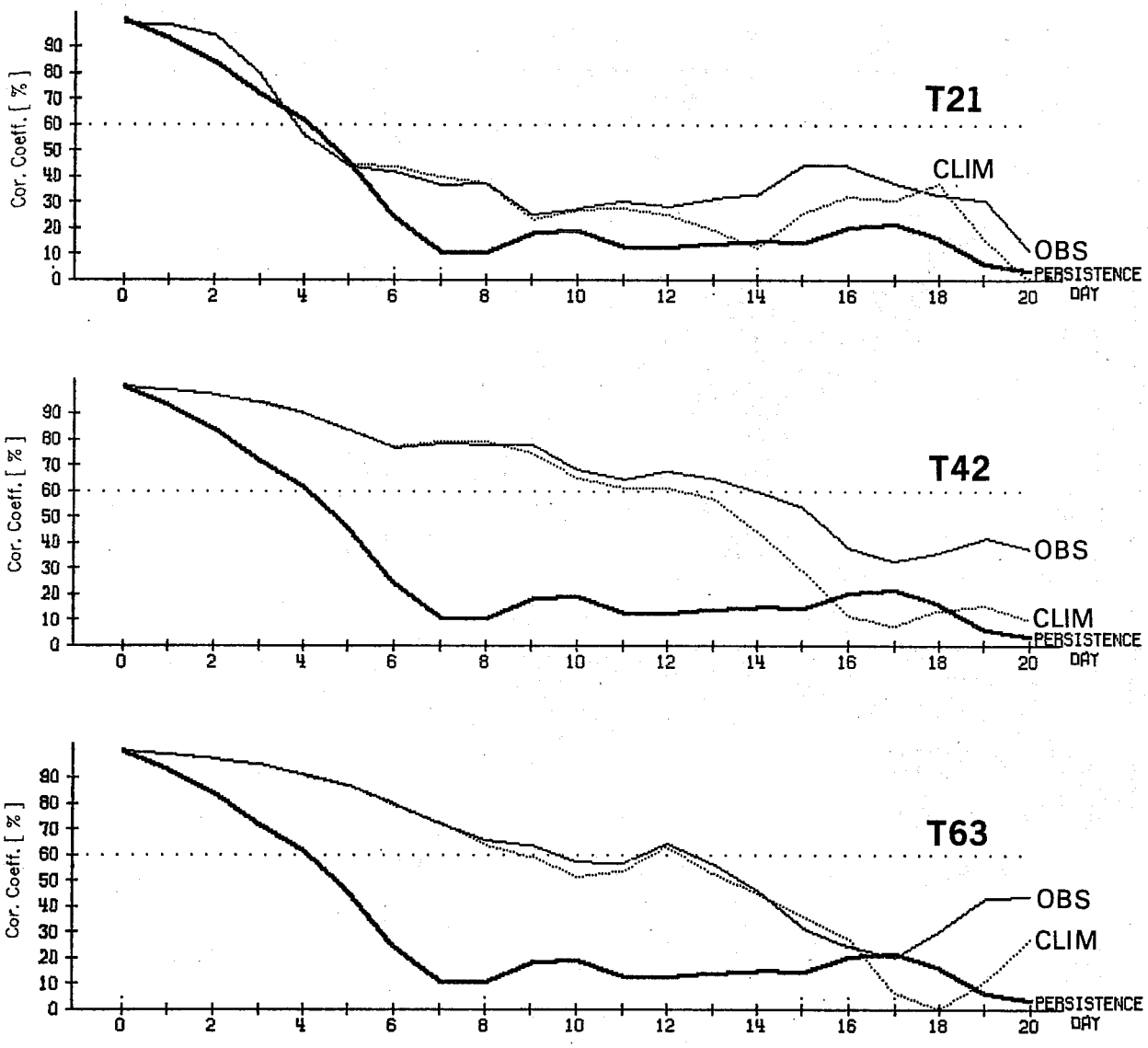

Fig.6: The anomaly correlation for the 500 mb height field and wavenumbers 1-3 in the latitude belt from 20.5 to 82.5°N for the FGGE case.

However, temperature deviations from climate of similar magnitude occur during that period at various locations so that the impact of the Atlantic anomaly cannot be isolated. In particular the temperature increase east of New Guinea seems to have the largest impact on the rainfall and might be the true cause for any change in the circulation because it is situated in a highly sensitive area (Simmons et al., 1983). The mean response will therefore not be discussed further for this case.

The single day scores (Fig. 6) show for the longest waves an improvement of predictability (as measured by the 60% anomaly correlation) of 24h with the T63 model when the observed SST is used; the T42 scores indicate a gain of about 36h in predictability. The more realistic boundary condition allows the correlation coefficient to stay above the 60% threshold up to about day 14, which is quite remarkable. It is not clear why the T42 model performs better than the higher resolution T63 model; it seems to be an exception rather than the rule (Jarraud et al., 1981). The T21 single day scores are hardly influenced by the SST.

For all resolutions the 10 day mean scores (Fig. 7) show an improvement in the first 10 to 20 days and, for all resolutions except T63, even up to day 20 to 30 for the cases with the observed SST. The limit of predictability (according to the definition mentioned above) is reached at day 15 for T21 and at day 25 for T42 and T63.

At the end of the forecasting period the correlation increases again reach more than 60% for the T21 experiment at day 50-60 and 48% for T63 at day 40-50; again the observed SST giving the better scores (except at T42). This increase in the scores can also be found in extended range experiments performed by other groups (Miyakoda and Crao, 1982). One simple explanation might be that the ultra-long waves have been predicted with a wrong negative

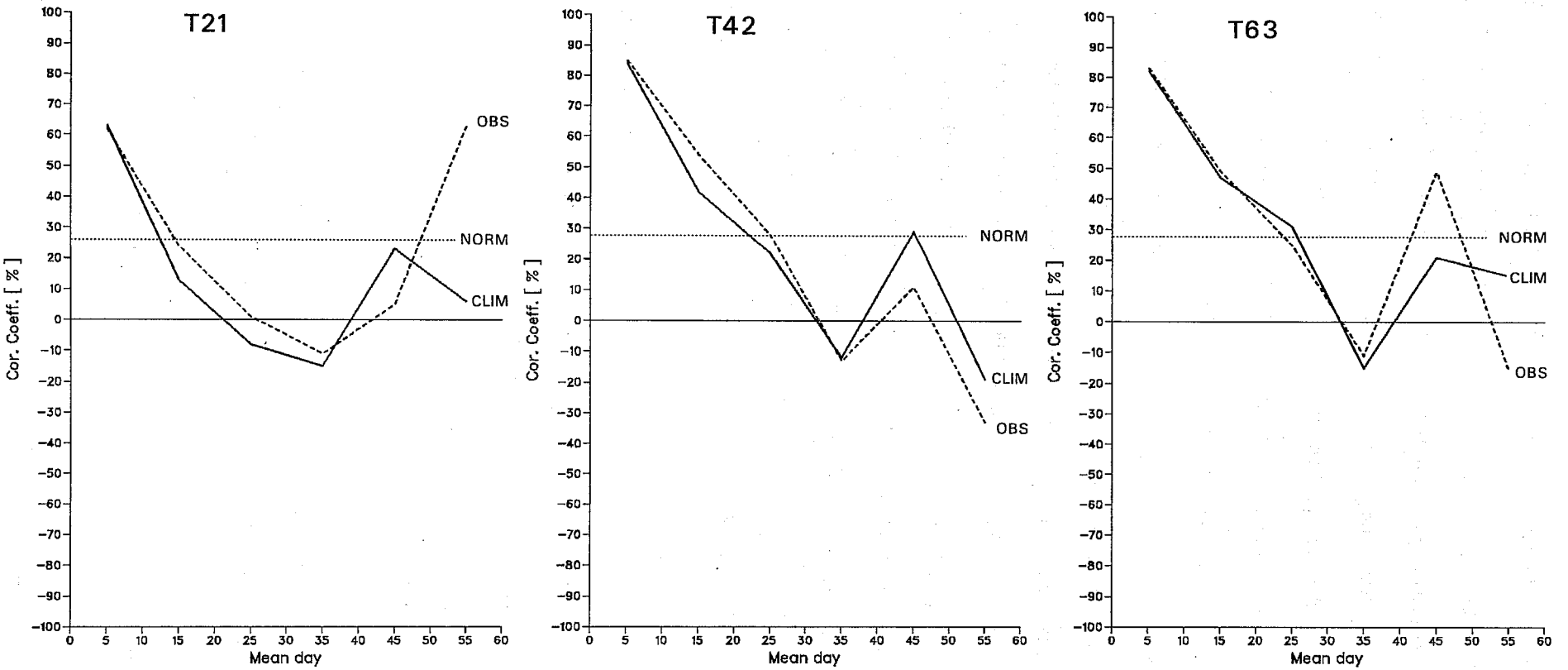

Fig.7: The 10 day mean anomaly correlation for the 500 mb height field for the FGGE case.

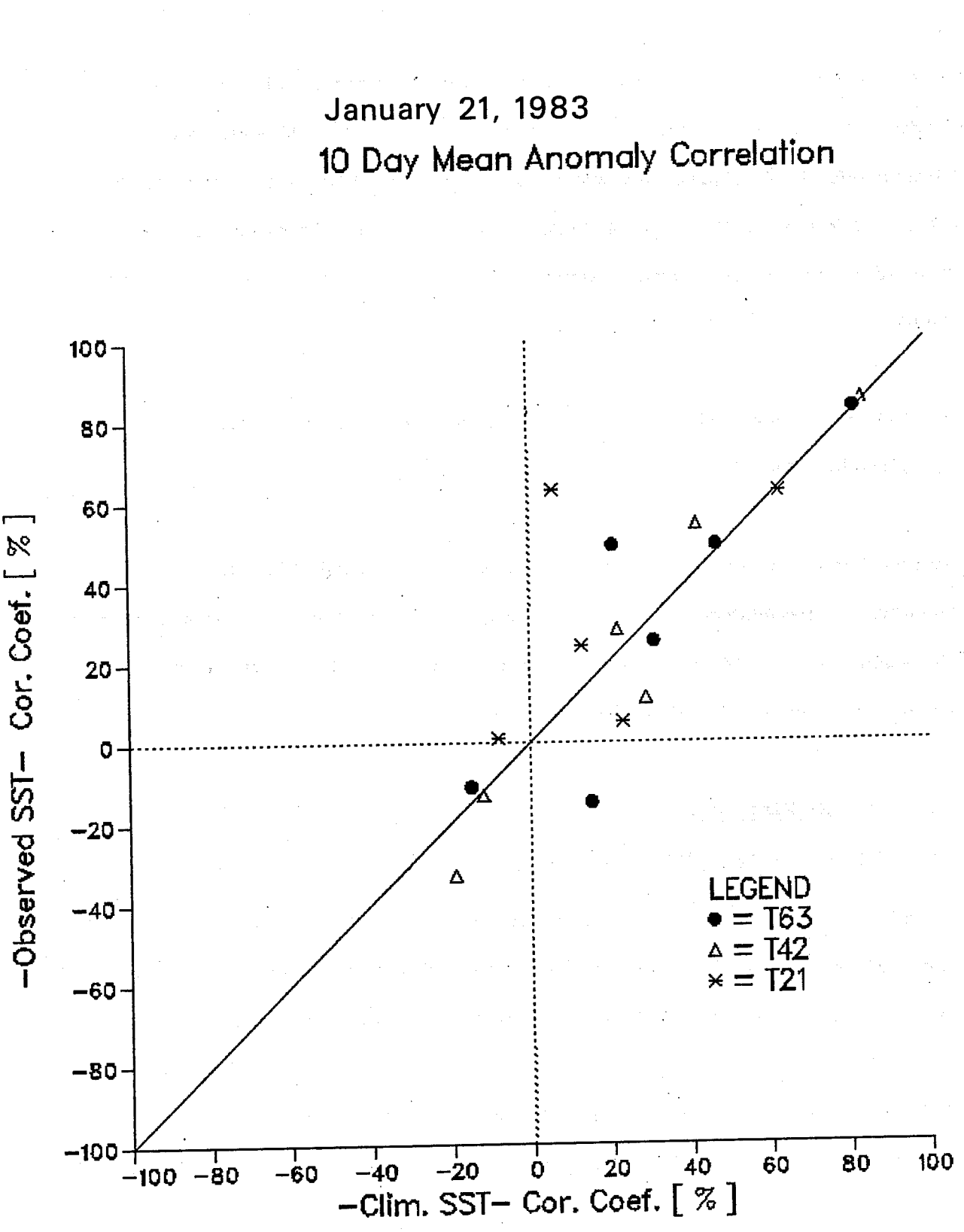

Fig.8: Intercomparison of the skill of the 10 day means from the experiments with observed and climatological SST for the FGGE case.

phase velocity. These waves would then have caught up with the observed long waves after a certain time. If a systematic error in the westward displacement takes place it would correspond to -8°longitude/day for T63, i.e. 7.2 m/s at 45°N. Against such a simple kinematic explanation is the fact that the control experiment does not show the recovery to the same extent.

The scatter diagram (Fig. 8) shows an improvement in the scores for the runs with the observed SST.

One has to conclude that a more realistic SST distribution has quite a beneficial impact on the quality of the forecast at the end of a medium range forecast, as well for extended range predictions. The effect seems to be larger for the higher resolution models.

4.2 The El Nino case

(a) Long term mean behaviour

In order to understand the results of this particular case it is necessary to investigate how well the anomaly is resolved at the various resolutions. As becomes clear from the temerature anomalies shown in Fig. 9, the interpolation to a T21 Gaussian grid reduces the observed maximum of the SST anomaly by about 1K, and even the T42 model experiences an underestimated temperature maximum. This fact has serious consequences for the strength and the location of the simulated rainfall, which is strongly dependent on the maximum of the absolute SST (Shukla, 1984, pers.com.). The rainfall (Fig. 10) increases for the T21 simulation only by about 17 mm/day for the anomaly run while it reaches 36 mm/day in a 40 day mean for T63. The location of the rainfall maximum for the higher resolution models is shifted towards the east.

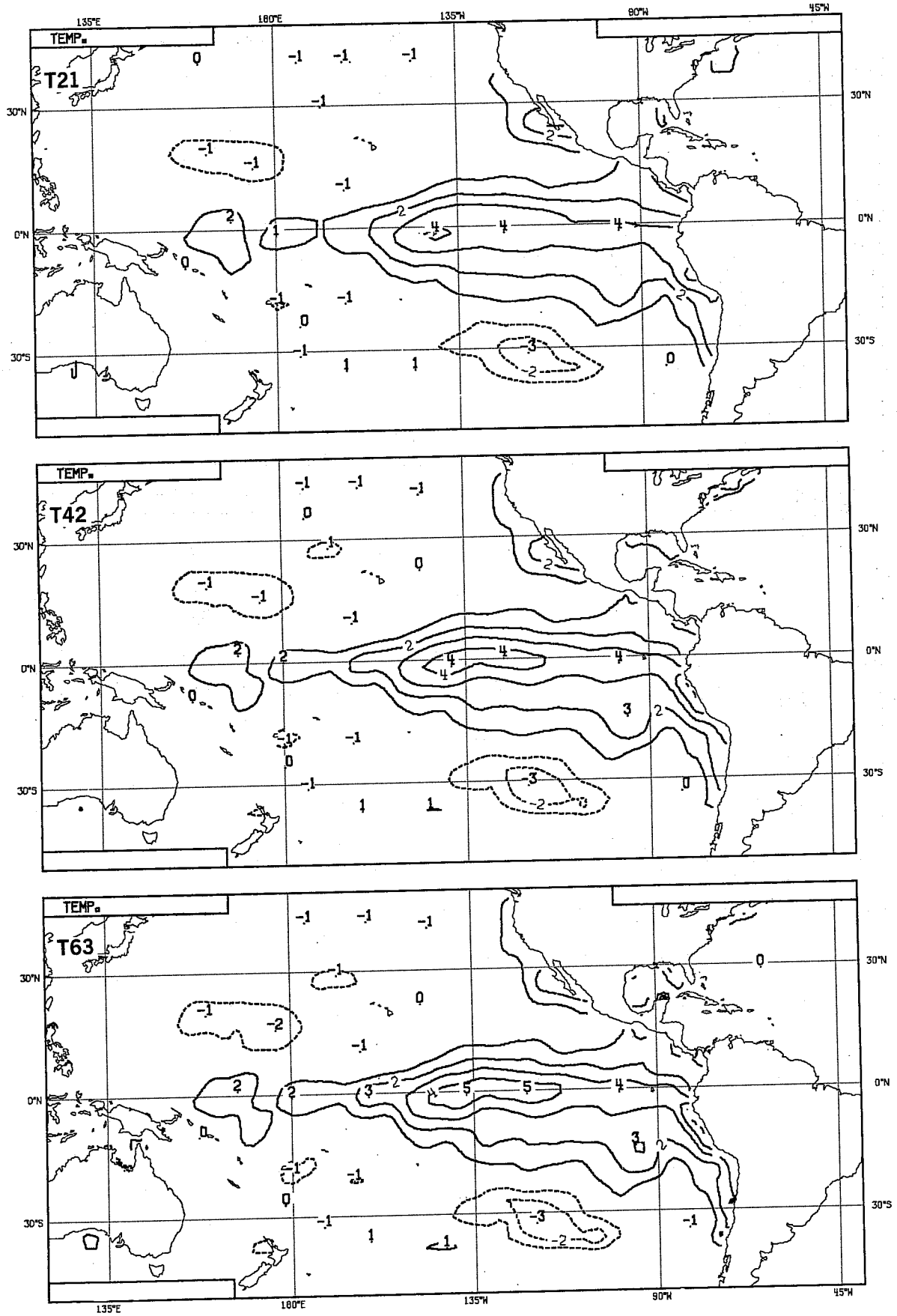

Fig.9: The observed El Nino anomaly as seen by the different resolutions (contour interval - 1°C).

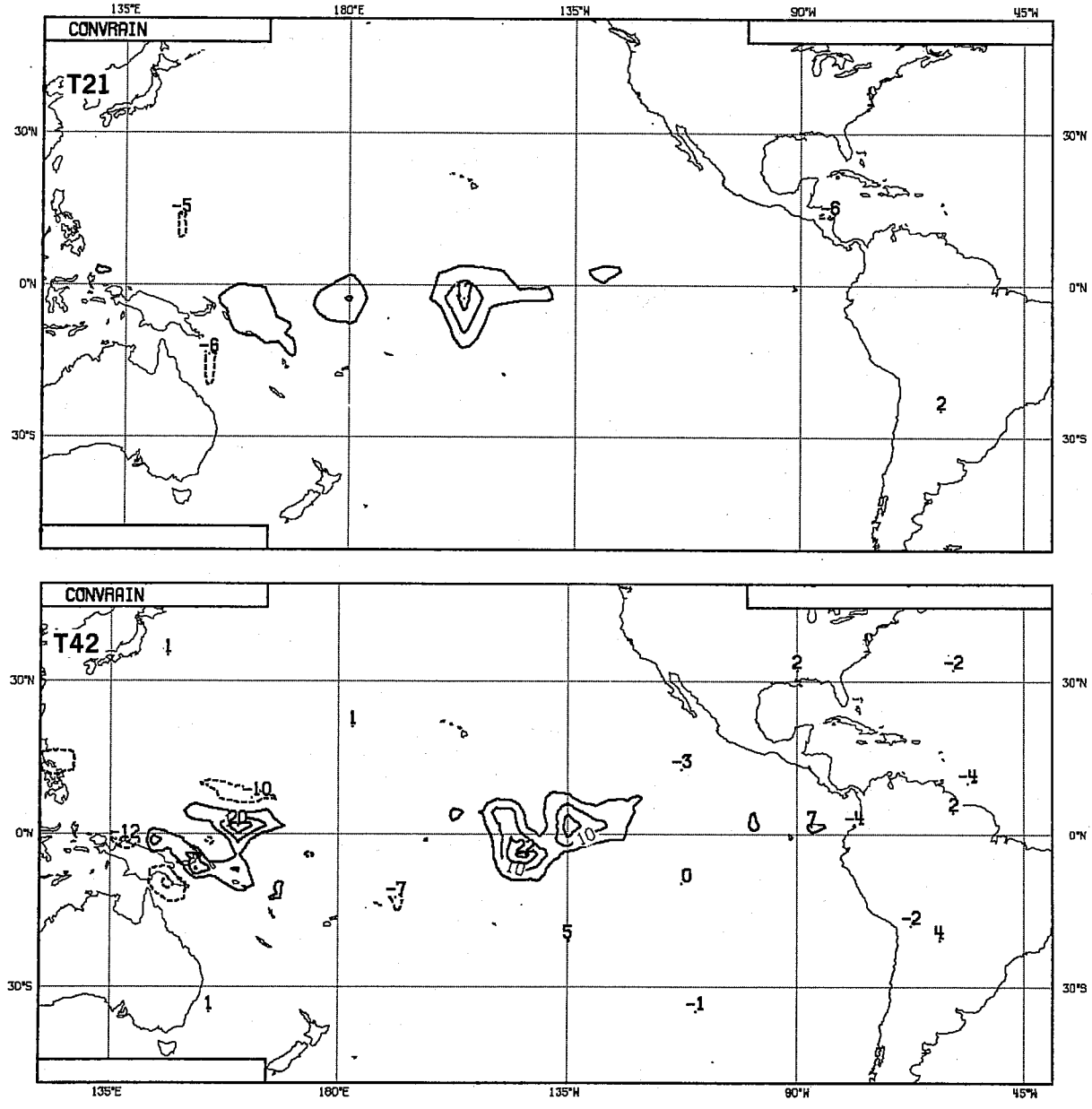

Fig.10: The difference between the precipitation from the experiment with the positive El Nino anomaly and the control (contour interval - 10 mm/day), and the observed outgoing longwave radiation anomaly (Arkin et al., 1983).

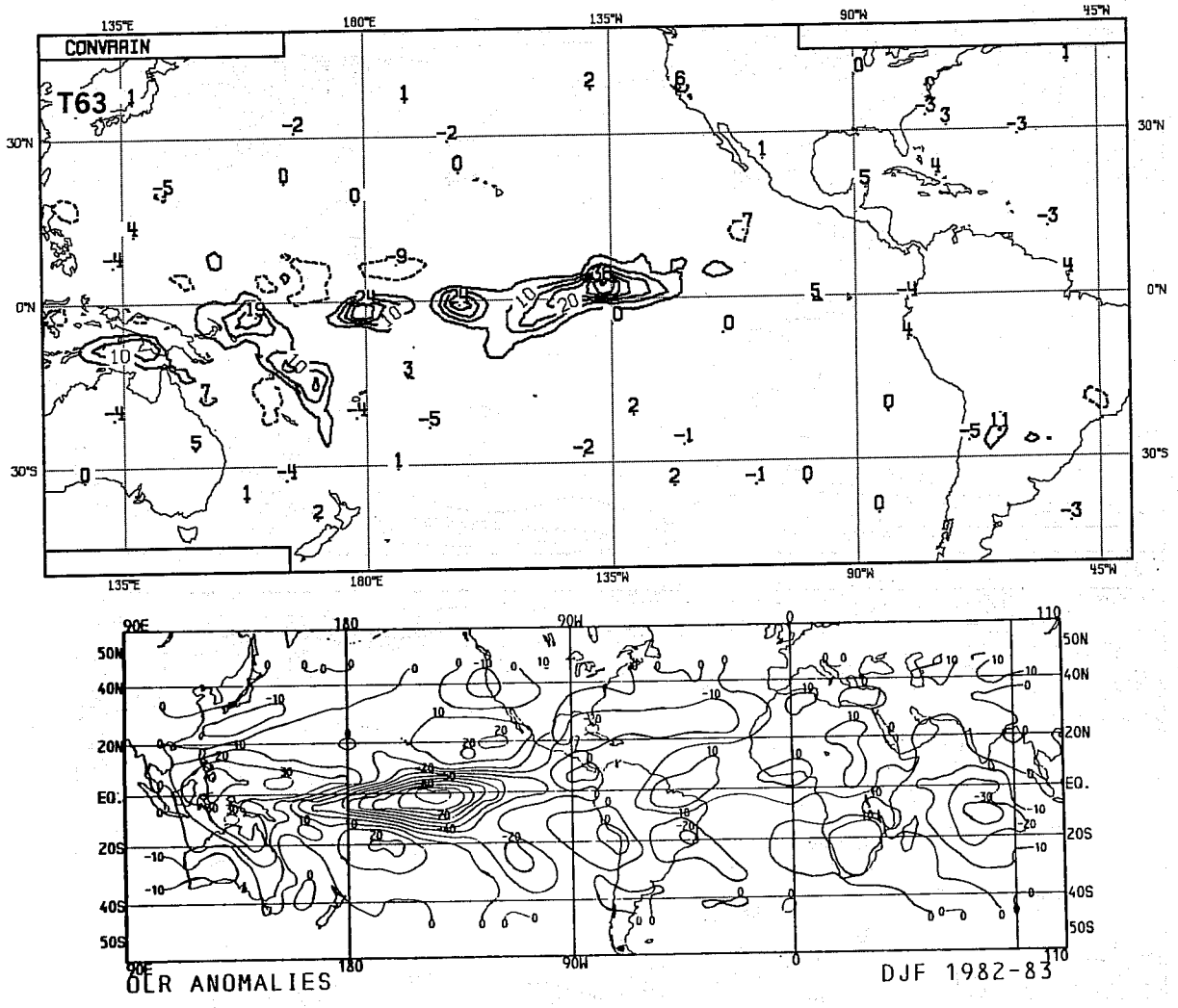

Fig.10: Continued.

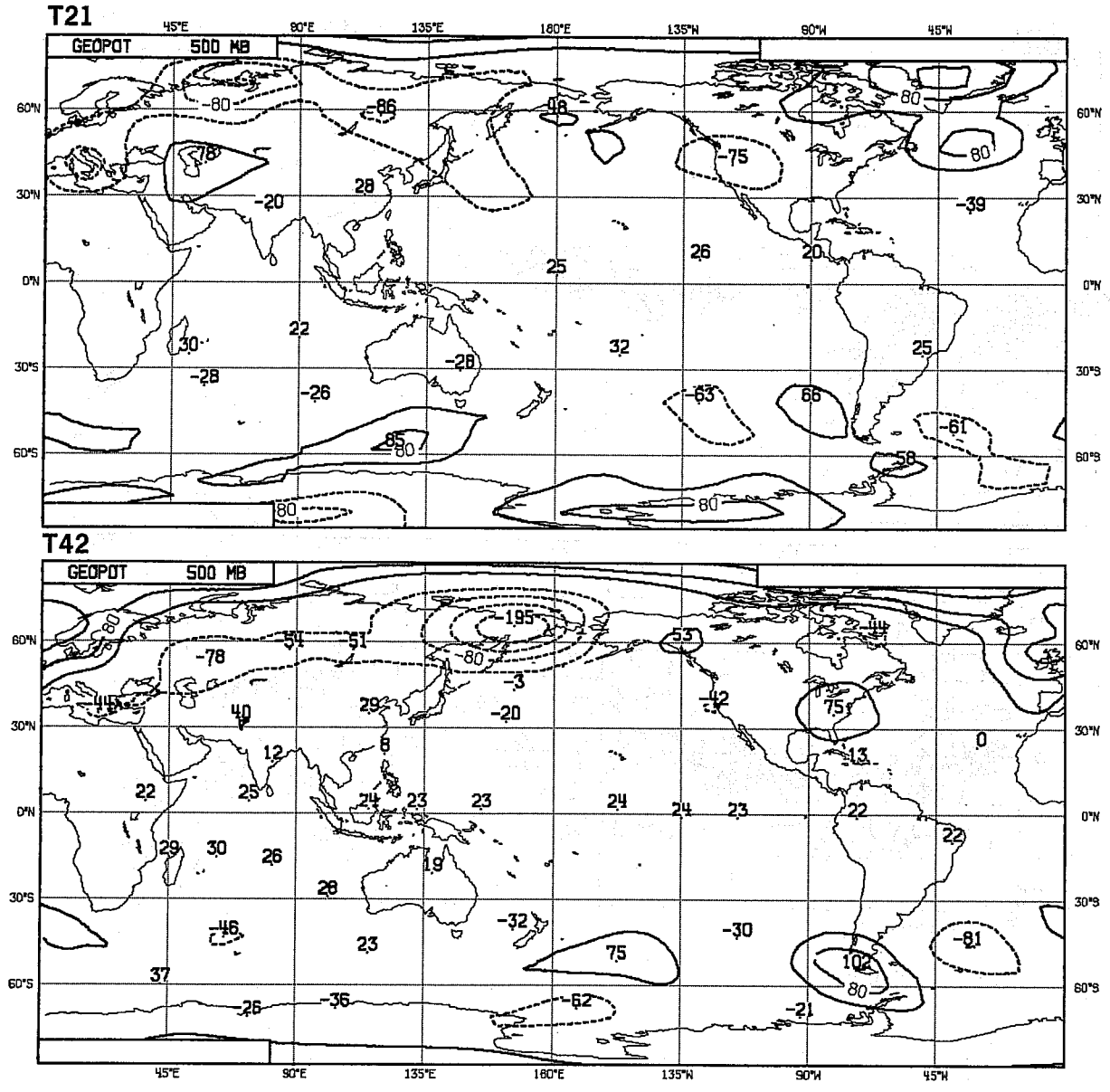

Fig.11: The anomaly of the 500 mb mean height field averaged for days 11 to 40 for the El Nino case (contour interval - 40 m).

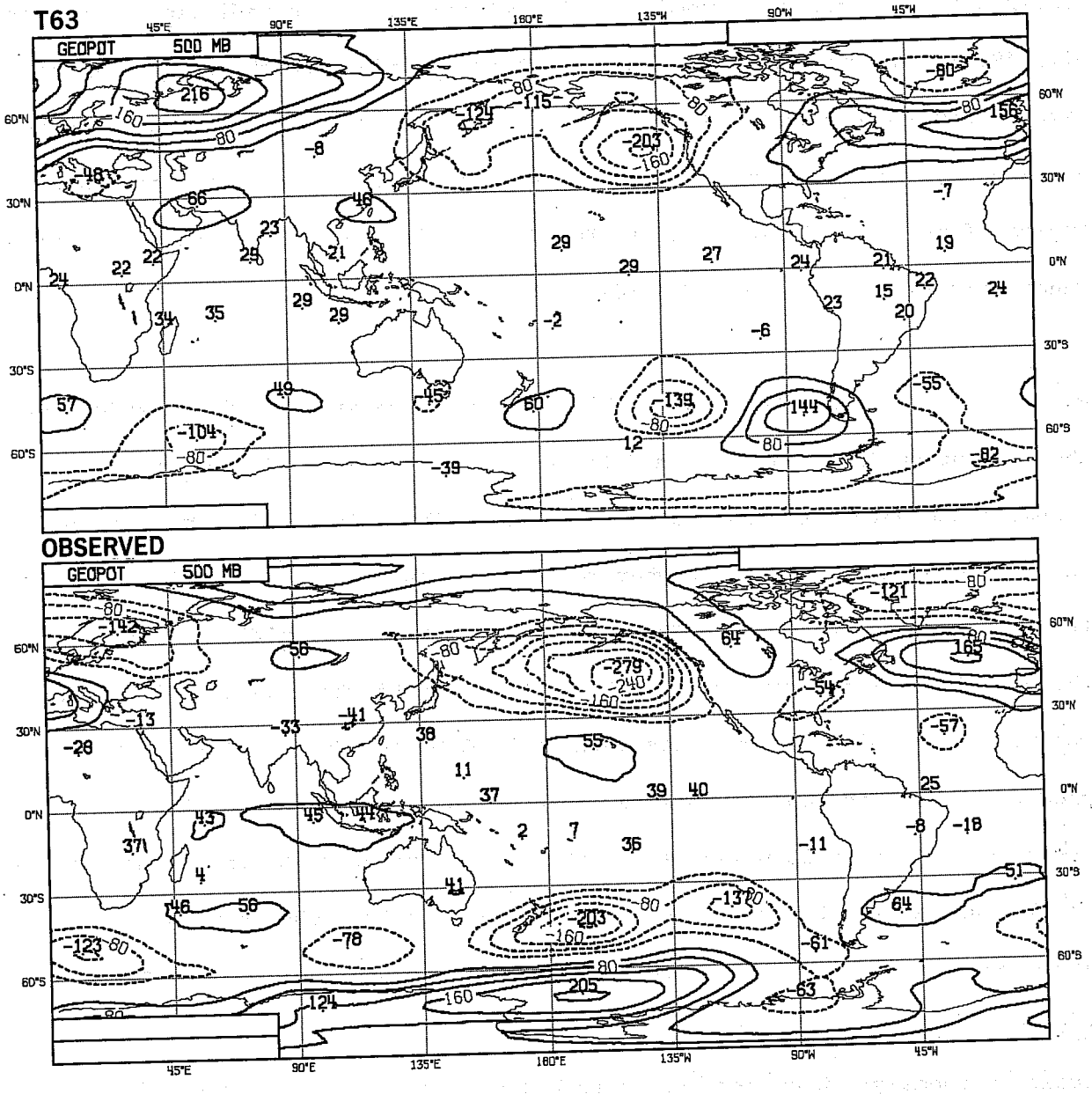

Fig.11: Continued.

Compared to the observed anomaly of the outgoing longwave radiation (Arkin et al., 1983), the rainfall band seems to be too confined to the equator in the simulations and a tail stretching from the equator eastwards to the southern hemisphere cannot be found in any simulations. The lack of this tail is a typical feature of the operational ECMWF model in the later stage of a medium range forecast (Molteni and Tibaldi, 1984).

As for the rainfall, the mean height field response is strongly dependent on the resolution (Fig. 11). In mid-latitudes the deviation in the 500 mb height field hardly exceeds 100m for the T21 simulation, while it is more than twice as large for the higher resolutions and appears to be largest with the highest resolution. The T63 and T42 integrations simulate a deepening of the Aleutian low and confirm the observations of Bjerknes (1966, 1969), as well as the results of long integrations by Cubasch (1984). The T21 model produces a weak region of pressure increase in this region and it is suspected that this is noise rather than a true response to the anomaly since it also appears in the run with the negative anomaly. The response for the T63 simulation is of larger extent than for any other resolution. The response to the negative anomaly is not the inverse of the one of the positive anomaly; it appears to be rather similar but with decreased amplitude. A similar reponse to a negative anomaly has been reported by Cubasch (1983).

The observed 500 mb height field anomaly for February 1983 bears an appreciable similartity to the T63 simulation for the northern hemisphere.

(b) Predictability

The impact of the SST anomaly on the predictablility appears to be small during the first 10 days for all resolutions for the single day anomaly correlations (Fig. 12). This confirms the results obtained by Arpe and

Wallace (1982). The T21 run recovers after about day 14 to reach a correlation of about 70% at day 18. Between day 10 and day 40 the T42 experiment shows no increase of the scores above 60%, while in the experiments with T63 the maximum correlation coefficient of about 65% is reached between days 28 and 30. This high scoring for T63 in the later part of the forecast must be more than mere coincidence since it happens only in the case with the observed positive anomaly, i.e. in the run with the most realistic boundary condition.

Up to day 15 the 10 day mean correlation (Fig. 13) decreases rapidly for all resolutions, but during the same period the runs with the observed anomaly score higher than the control experiments, which in turn score higher than the experiments with the negative anomaly as long as the score do not drop below the threshold values defined in Section 3.2. The T21 experiments stay above this threshold for almost all the forecast, while the T42 goes below it at about day 16 for the control and at about day 22 for the case with the observed anomaly. The T63 control experiment looses its predictability at around day 13 while the experiment with the El Nino anomaly just reaches the threshold value, but stays above it for the rest of the forecast. The difference in the correlation between the T63 control experiment and the anomaly experiment is about 30%.

To illustrate this difference the 500 mb height anomaly between day 21 and 30 have been displayed together with the observed anomaly in Fig. 14. In the simulations over Europe, an area with large height field anomalies can be found. These are a reflection of the tendency of the model to zonalize the flow. However, the simulation with the SST anomaly generates a decrease of pressure in the north east Pacific and a rise of the pressure over Europe, which coincides with observed pressure anomalies. A similar response of the

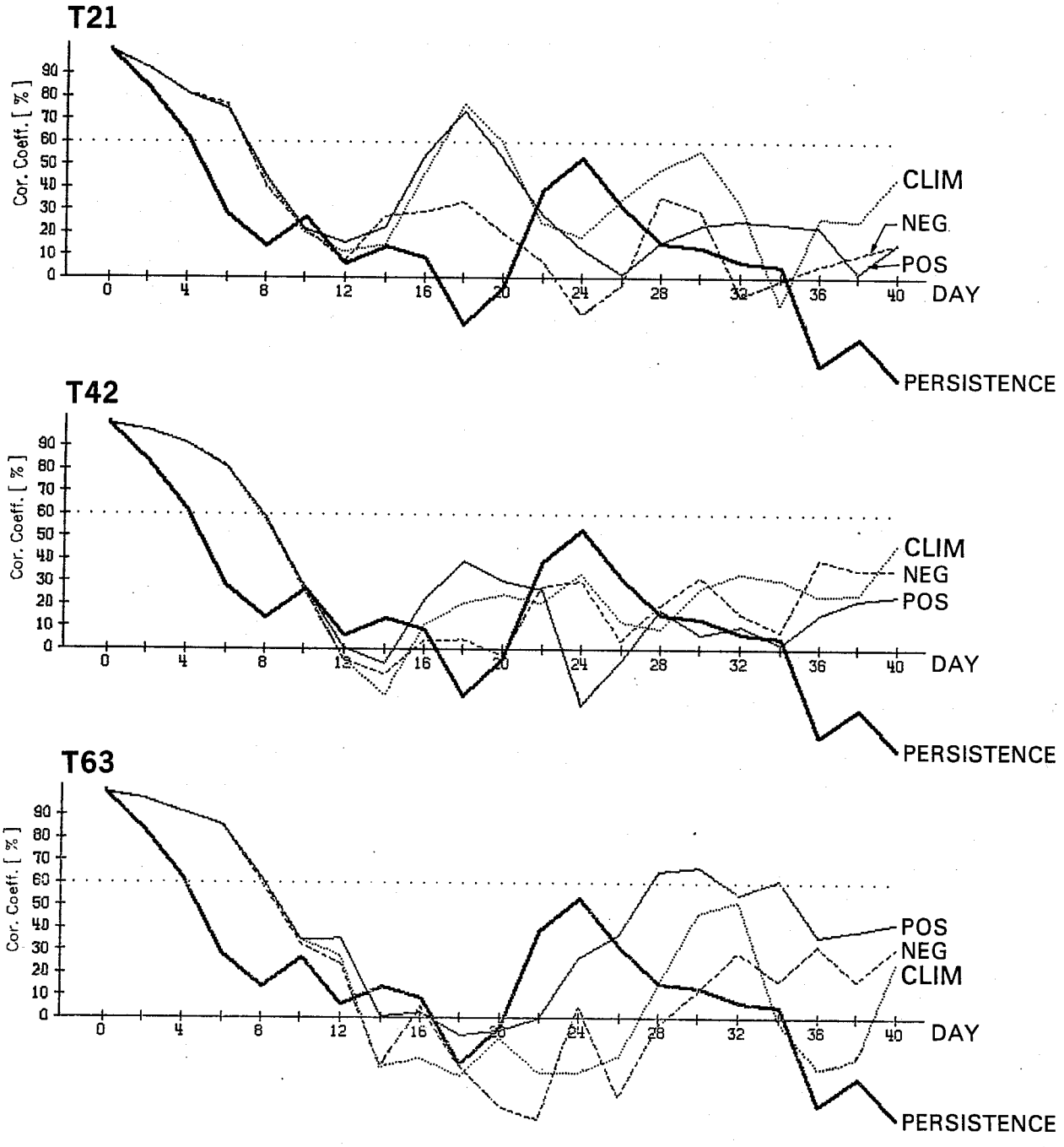

Fig.12: The anomaly correlation for the 500 mb height field and wavenumbers 1-3 in the latitude belt from 20.5 to 82.5°N for the El Nino case.

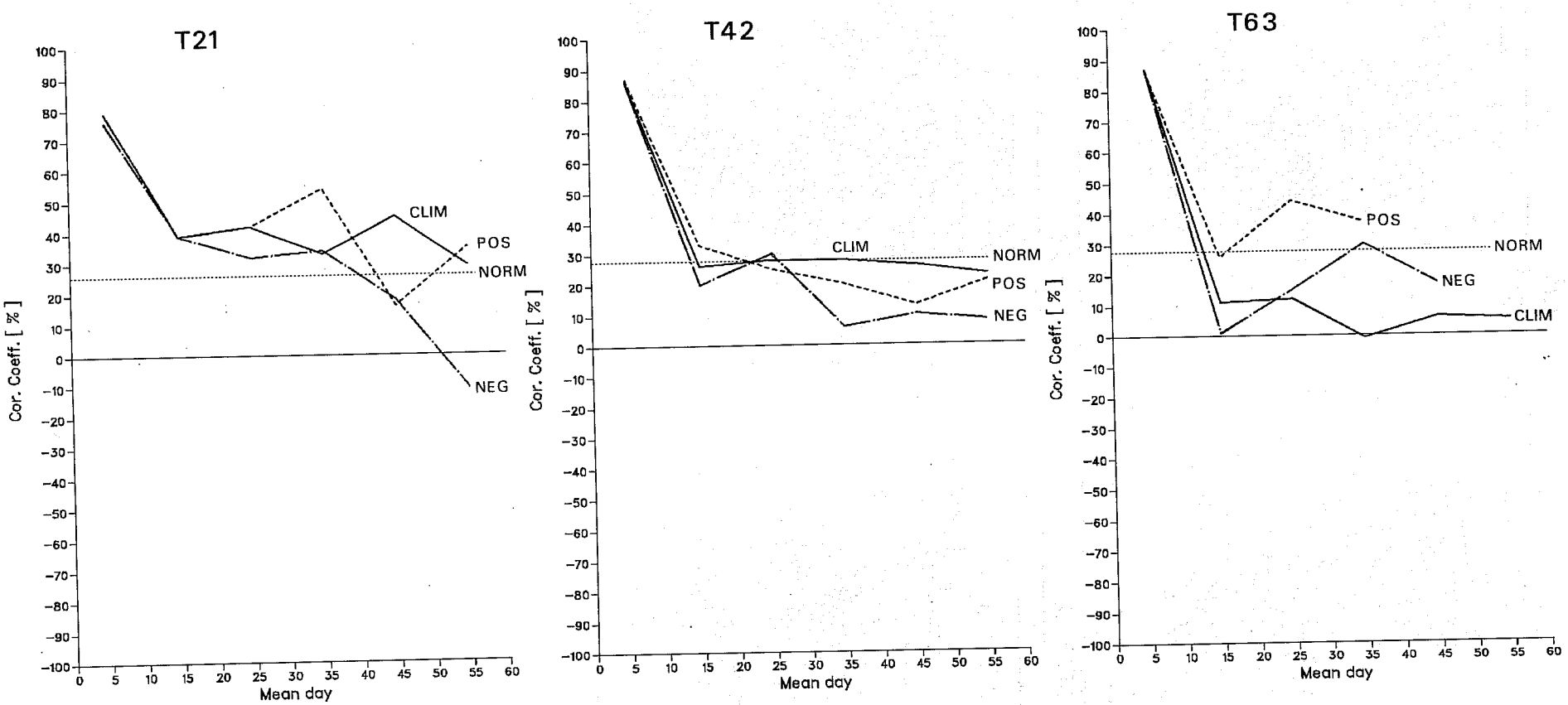

Fig.13: The 10 day mean anomaly correlation for the 500 mb height field for the El Nino case.

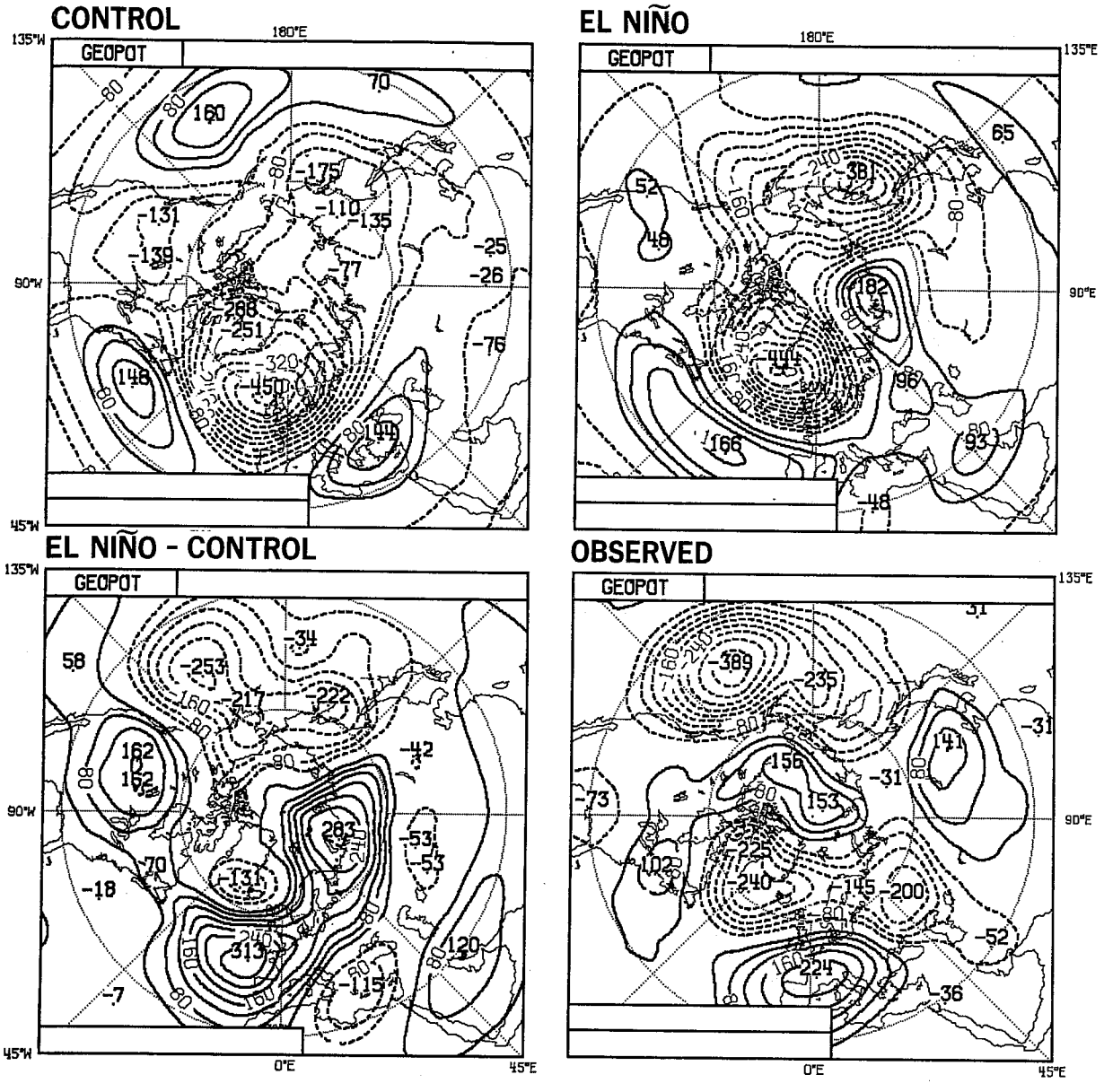

Fig.14: The 500 mb mean height field anomaly for the El Nino case averaged for days 21 to 30 (contour interval - 40 m); resolution: T63.

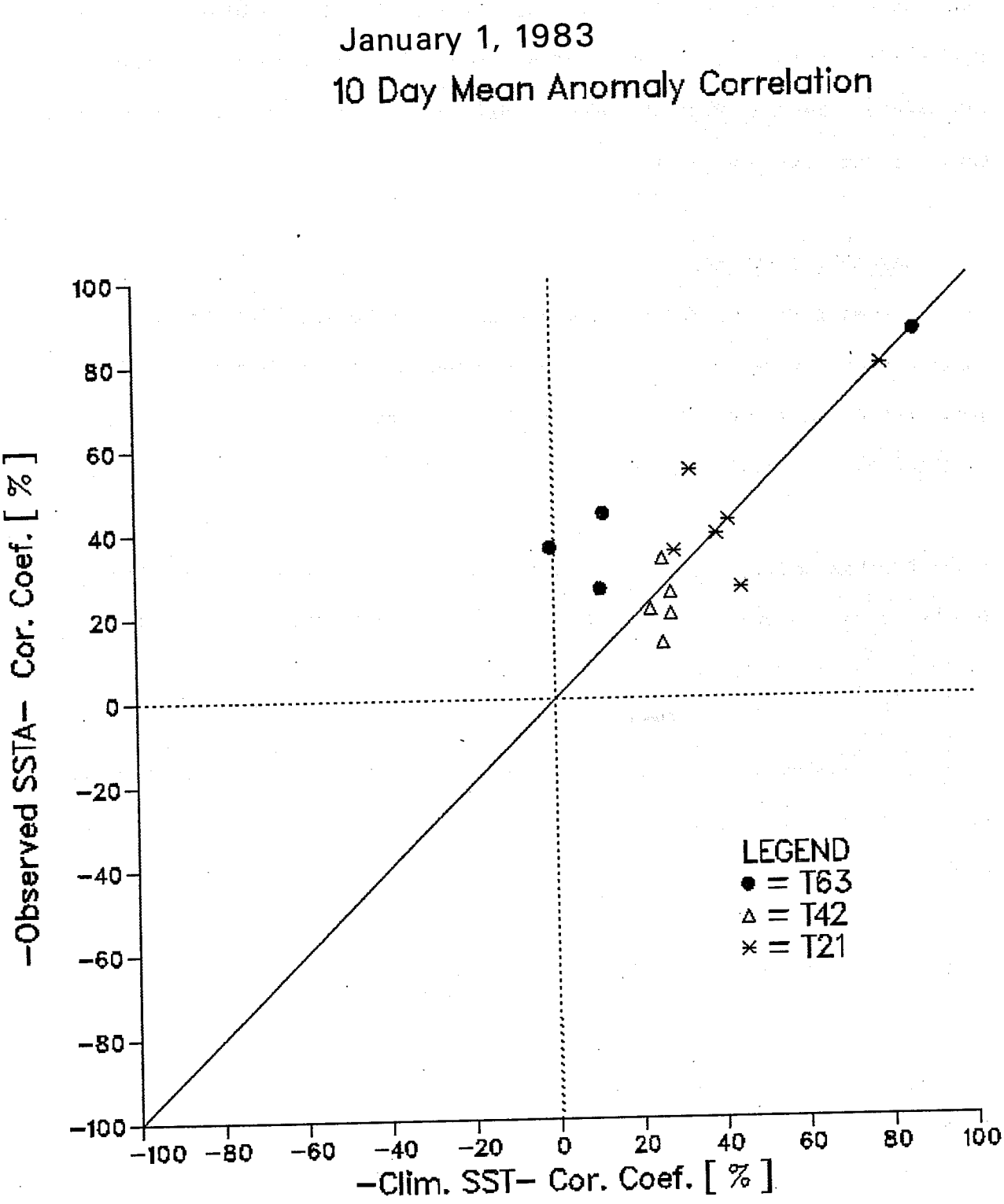

Fig.15: Intercomparison of the skill of the 10 day means between the experiments with the positive anomaly and the climatological SST for the El Nino case.

model atmosphere had been found by Cubasch (1984) and resembles, at least in the Pacific region, the response of a linear model to tropical forcing. The scatter diagram (Fig. 15) shows a distinct improvement for the runs with the more realistic SST anomaly.

5. CONCLUDING REMARKS

Before summarizing the SST experiments it has to be stressed that all results apply for single case studies and their general validity has still to be established. However, they give some hints as to which direction such investigations should proceed.

- The SST has an impact on the forecast in mid-latitudes which becomes more important as the prediction progresses. The impact during the first 10 days seems to be only marginal.

- The low resolution model has some difficulties in resolving SST anomalies. The impact of SST anomalies is therefore easier to detect in high resolution models.

- The skill score of almost all experiments is higher when a more realistic SST distribution is used.

- The skill score of the experiments increases after about 15 days and can reach the level of direct predictability (i.e. a correlation coefficient of more than 60%). This means that some forecasts show predictive skill between day 20 to 30, even though they did not have any skill between day 10 to 20. The reasons behind this behaviour are not known, but it appears to be systematic and can also be found in similar studies of other groups. It is more pronounced using a more realistic SST distribution.

• The usable information contained in extended range predictions is obscured the flow being too zonal. This zonalization becomes worse with increased resolution. It seems, however, to approach an asymptotic value. The T63 model climate is therefore about as zonal as that of a T42 model simulation.

REFERENCES

Alexander, R.C. and R.L.Mobley, 1974: Monthly average sea surface temperatures and ice pack limits on a 1 degree global grid. Rand Report R 1310-ARPA.

Arkin, P.A., J.D.Kopman and R.W.Reynolds, 1983: 1982/83 El Nino/Southern Oscillation event quick look atlas. NOAA/National Weather Service, NMC/CAC, Washington, D.C.20233.

Arpe, K.and J.M.Wallace, 1982: Tropical Pacific sea-surface temperature anomaly experiments with the ECMWF medium range forecast model. Proceedings 7th climate diagnostics workshop, NOAA, 340-348.

Bengtsson, L., 1981: Numerical prediction of atmospheric blocking - a case study. Tellus, 33, 19-42.

Bjerknes, J., 1966: A possible response of the atmospheric Hadley circulation to the equatorial anomalies of the ocean temperature. Tellus, 18, 820-829.

Bjerknes, J., 1969: Atmospheric teleconnections from the equatorial Pacific. Mon.Wea.Rev., 87, 163-172.

Cubasch, U., 1983: Sensitivity of the ECMWF model to changes in resolution. ECMWF Workshop on "Intercomparison of large scale models used for extended range forecasts". 30 June-2 July 1982, ECMWF, Shinfield Park, Reading, UK, 435-453.

Cubasch, U., 1984: The mean response of the ECMWF global model to the El Nino anomaly in extended range prediction experiments. Atmosphere-Ocean. (Accepted for publication).

Hollingsworth, A., K.Arpe, M.Tiedtke, M.Capaldo and H.Savijaervi, 1980: The performance of a medium-range forecast model in winter: Impact of physical parameterizations. Mon.Wea.Rev., 108, 1736-1773.

Jarraud, M., C.Girard and U.Cubasch, 1981: Comparison of medium range forecasts made with models using spectral or finite difference techniques in the horizontal. Techn.Rep.No.23, ECMWF, Shinfield Park, Reading, UK.

Louis, J.-F., (Editor), 1984: The ECMWF forecasting model - physical parameterisation. ECMWF Research Manual Vol.3, ECMWF, Shinfield Park, Reading, U.K.

Miyakoda, K.and J.-P.Crao, 1982: Essay on dynamical long-range forecasts of atmospheric circulation. J.Met.Soc.Japan, 60, 292-307.

Molteni, F.and S.Tibaldi, 1984: Climatology and systematic error of the ECMWF rainfall forecast. Tech.Rep.in preparation, ECMWF, Shinfield Park, Reading, UK.

Reynolds, R.W., 1984: The 1982/83 El Nino sea surface temperatures. NOAA Climate Analysis Centre, NMC, Washington D.C., USA.

Shukla, J., and J.M.Wallace, 1983: Numerical simulation of the atmospheric response to equatorial Pacific sea surface temperature anomalies. J.Atmos.Sci., 40, 1613-1630.

Simmons, A.J., J.M.Wallace and G.W.Branstator, 1983: Barotropic wave propagation and instability and atmospheric teleconnection patterns. J.Atm.Sci., 40, 1363-1392.

Tibaldi, S. and J.-F.Geleyn, 1981: The production of a new orography, land-sea mask and associated climatological surface fields for operational purposes. ECMWF Tech.Memo.No.4, ECMWF, Shinfield Park, Reading, U.K.

v.Storch, H., E.Roeckner and U.Cubasch, 1984: Intercomparison of extended range January simulations: Statistical assessment of ensemble properties. Submitted to Beitr.Phys.Atmos.